Available online at website: https://journal.bcrec.id/index.php/bcrec

Bulletin of Chemical Reaction Engineering & Catalysis, 20 (2) 2025, 331-345

Original Research Article

Modeling Syngas Fermentation for Ethanol Production under Fluctuating Inlet Gas Composition

Noviani Arifina Istiqomah[1], Rendy Mukti[2,], Made Tri Ari Penia Kresnowati[2,3*], Tjandra Setiadi[2]**

[1]Doctoral Program of Chemical Engineering, Faculty of Industrial Technology, Institut Teknologi Bandung, Indonesia
[2]Department of Chemical Engineering, Faculty of Industrial Technology, Institut Teknologi Bandung, Indonesia
[3]Department of Food Engineering, Faculty of Industrial Technology, Institut Teknologi Bandung, Indonesia

Received: 17th March 2025; Revised: 18th April 2025; Accepted: 21th April 2025
Available online: 24th April 2025; Published regularly: August 2025

Abstract

Syngas fermentation effectively converts CO, H_2, and CO_2 into valuable biofuels and chemicals. This study investigated the effects of fluctuating syngas composition and kLa as the critical operational parameters on microbial fermentation performance, with a focus on ethanol, acetic acid, and biomass production. Modeling results demonstrated that increasing CO concentration significantly enhanced metabolite production, whereas increases in H_2 and CO_2 concentrations yielded limited improvements. The findings revealed that a higher H_2/CO ratio tent to reduce metabolite production, while a higher CO/CO_2 ratio significantly improved fermentation outcomes. Additionally, higher kLa values were observed to promote metabolite production, though diminishing returns were evident at very high kLa levels. Further study on the impact of syngas composition disturbances (±5% to ±20%) and fluctuation durations (0.5, 1, 2, and 4 days) indicated that larger disturbances and longer fluctuation durations led to greater deviations in metabolite concentrations, with ethanol being the most sensitive, followed by acetic acid and biomass. Despite these fluctuations, the microbial system displayed resilience, stabilizing once gas composition returned to normal levels. These insights underscored the adaptability and robustness of syngas fermentation systems, making them viable for industrial applications where gas composition variability is inevitable. The ability to tolerate moderate fluctuations offers opportunities to reduce gas pretreatment costs and process syngas from diverse sources, benefiting industries such as steel manufacturing, oil refining, and biomass gasification.

Keywords: Ethanol Production; Inlet Gas Composition Fluctuation; kLa; Model Simulation; Syngas Fermentation

How to Cite: Istiqomah, N. A., Mukti, R., Kresnowati, M. T. A. P., Setiadi, T. (2025). Modeling Syngas Fermentation for Ethanol Production under Fluctuating Inlet Gas Composition. *Bulletin of Chemical Reaction Engineering & Catalysis*, 20 (2), 331-345. (doi: 10.9767/bcrec.20369)

Permalink/DOI: https://doi.org/10.9767/bcrec.20369

Supporting Information (SI): https://journal.bcrec.id/index.php/bcrec/article/downloadSuppFile/20369/5691

1. Introduction

Global demand for fossil fuels has surged alongside population growth [1,2]. Biofuel production, especially ethanol from lignocellulose, follows two primary pathways: biochemical and thermochemical [3–5]. In the biochemical pathway, biomass undergoes pretreatment with acid, alkali, or steam to disrupt the cellulose-hemicellulose-lignin bond, enhancing its accessibility to enzymes. This pretreated biomass is then hydrolyzed to produce fermentable sugars, which are fermented to yield ethanol [6]. The biochemical pathway offers high selectivity of biocatalyst products [7], a relatively simple reactor design, and the ability to operate at ambient temperature and pressure [8]. However, it also faces challenges, including high costs for

* Corresponding Author.
Email: kresnowati@itb.ac.id (M.T.A.P. Kresnowati)
** Present address: Department of Chemical Engineering, Faculty of Engineering and Agricultural, Universitas Setia Budhi Rangkasbitung, Indonesia

pretreatment and enzymes, a slower process, and the production of lignin as a by-product. Additionally, pretreatment can release inhibitory compounds (such as acetic acid, furfural, 5-hydroxymethylfurfural, and phenolic compounds) that may hinder hydrolysis and fermentation [9,10].

The thermochemical pathway converts biomass into syngas (a mixture of CO and H_2) [11–13], which is then transformed into biofuels using the Fischer-Tropsch (FT) catalyst. The FT process can utilize various raw materials, including lignin, and operates quickly. However, it faces challenges such as substantial infrastructure requirements, high metal catalyst costs, and the necessity for elevated temperatures, pressures, consistent gas quality, and a stable CO/H_2 ratio [14].

The third pathway, syngas fermentation, integrates the benefits of biochemical and thermochemical methods. Biomass feedstock is first thermochemically converted into syngas, which then serves as the carbon source for microbial biocatalysts that produce ethanol [15]. Potential microbes for this process are acetogenic bacteria capable of converting organic acids into alcohol [16], such as *Clostridium ljungdahlii, Clostridium autoethanogenum, Clostridium carboxidivorans P7*, and *Acetobacterium woodii* [17]. Acetogens can utilize H_2, CO, sugars, one-carbon compounds, methoxylated aromatic compounds, and alcohols [18].

Microbes convert syngas into metabolic products via the Wood-Ljungdahl pathway, also known as the reductive acetyl-CoA pathway [19]. The fermentation process consists of two stages: acidogenesis and solventogenesis [20]. During acidogenesis, cell growth occurs alongside the production of acetate and butyrate, while in solventogenesis, these products are transformed into ethanol. Thermodynamically, producing ethanol and acetic acid from CO is more favorable than using CO_2 and H_2, as CO_2 requires H_2 to serve as a substrate [21]. However, CO's solubility in aqueous solutions is much lower than that of CO_2 [22].

Syngas fermentation success depends on the microorganism used for ethanol production, the bioreactor type for gas-liquid mass transfer, and syngas composition [23]. Syngas fermentation offers an advantage over chemical processes by not relying on a fixed H_2/CO ratio, as acetogenic bacteria can adapt their metabolic pathways to different ratios [24,25]. However, varying H_2/CO ratios may lead to fluctuations in bioethanol productivity.

Syngas composition varies due to biomass feedstock composition, gasifier, gasification agent, and process temperature [26]. However, in syngas fermentation for ethanol production research often a constant syngas substrate composition was used. In developing countries, the applied simple gasification methods and the use of various biomass types can result in inconsistent syngas compositions, affecting microbial conversion efficiency in syngas fermentation. In large-scale syngas fermentation, changes in dissolved gas concentrations (CO, H_2, CO_2) are likely due to local differences in mass transfer and convection rates [27–31]. Research indicates that H_2/CO ratio variations affect fermentation outcomes: a ratio of 2.0 yields more acetate than ethanol, while a ratio of 0.5 favors ethanol production [32]. This variability in gas composition raises concerns regarding the effectiveness of microorganisms in converting syngas to desired products.

Laboratory experiments are crucial for assessing how changes in syngas composition influence metabolism, but they demand significant resources. Model simulation can be used to predict fermentation dynamics to address the effect of fluctuations in syngas composition. This research investigates the impact of syngas composition on batch fermentation and analyzes how fluctuations and disturbances in syngas composition affect continuous fermentation through modeling. Key parameters include cell concentration, ethanol levels, acetic acid, and gas utilization (CO, CO_2, and H_2). The experiment employs a kinetic model to examine how syngas variability influences fermentation efficiency, focusing on factors such as mass transfer rate (kLa), fluctuation of syngas composition, and duration of fluctuations.

This study highlited the significance of understanding how fluctuations in inlet gas composition affect the optimization of the syngas fermentation process, particularly in the use of CO_2 and CO, as well as the production of biomass, ethanol, and acetate. Improving the efficiency of syngas fermentation can lead to cleaner energy alternatives, reduced greenhouse gas emissions, and the promotion of bio-based products, all of which are crucial for transitioning to a low-carbon economy and advancing sustainable industrial practices.

2. Methods

The built model includes dissolution of CO, CO_2, and H_2 gas from the feed gas into the liquid medium of the fermentation broth, the conversion of dissolved CO and CO_2/H_2 into acetate and biomass (acetogenesis phase), the process of converting acetate into ethanol (solventogenesis phase). *Clostridium ljungdahlii* produces acetic acid and biomass following a growth-associated mechanism during the acetogenesis phase and produces ethanol following a non-growth-associated mechanism during the solventogenesis phase. Ethanol can also be formed along with biomass growth following the mix-growth-associated mechanism.

The model for the batch system (Figure 1a) examines the effects of *kLa* and syngas composition changes on fermentation. Additionally, the model is simulated continuously (Figure 1b) to analyze the impacts of fluctuation magnitude and duration in the inlet gas composition on fermentation. Both systems operate under the same reaction kinetics and liquid medium composition, including gas flow and agitation rates.

The assumptions of this simulation are as follows: (1) The simulation employs a kinetic model developed by Medeiros *et al.* [33] in which kinetic parameters were fitted from Phillips *et al.* [34]; (2) The kinetic equation includes 11 variables: $CO_{(g)}$, $CO_{(l)}$, $CO_{2(g)}$, $CO_{2(l)}$, $H_{2(g)}$, $H_{2(l)}$, ethanol$_{(g)}$, ethanol$_{(l)}$, acetate$_{(g)}$, acetate$_{(l)}$, and biomass; (3) The effects of synthesis gas composition and $k_L a$ on batch fermentation were analyzed over 14 days to ensure its effects solventogenesis and acetogenesis processes were covered; (4) The process is assumed to operate isothermally and isobarically, with constant homogeneity and volume of liquid and gas in the reactor; (5) The influence of variations in syngas composition fluctuations during fermentation varies according to the magnitude of the disturbance and the duration of the disturbance analyzed for 16 days starting on the day of fermentation operations producing ethanol and acetic acid at steady state conditions on continue fermentation.

The kinetic model adheres to the stoichiometry of reactions 1–4, which represent cell-catalyzed chemical reactions:

$$4\ CO + 2\ H_2O \rightarrow CH_3COOH + 2\ CO_2 \quad (1)$$
$$4\ H_2 + 2\ CO_2 \rightarrow CH_3COOH + 2\ H_2O \quad (2)$$
$$CH_3COOH + 2\ CO + H_2O \rightarrow C_2H_5OH + 2\ CO_2 \quad (3)$$
$$CH_3COOH + 2\ H_2 \rightarrow C_2H_5OH + 2\ H_2O \quad (4)$$

The specific consumption rate CO (v_{CO}) and H_2 (v_{H_2}) follow Monod kinetics with inhibition by substrate and product (Equations 5 and 6). $C_{L,CO}$ is concentration of CO in the liquid phase. $C_{L,H2}$ is concentration of H_2 in the liquid phase. The values of maximum specific consumption rates of CO and H_2 ($v_{\max\ CO}$ ($v_{max,H2}$) and the Monod constants ($K_{S,CO}$ *dan* $K_{S,H2}$) are taken from Medeiros [35].

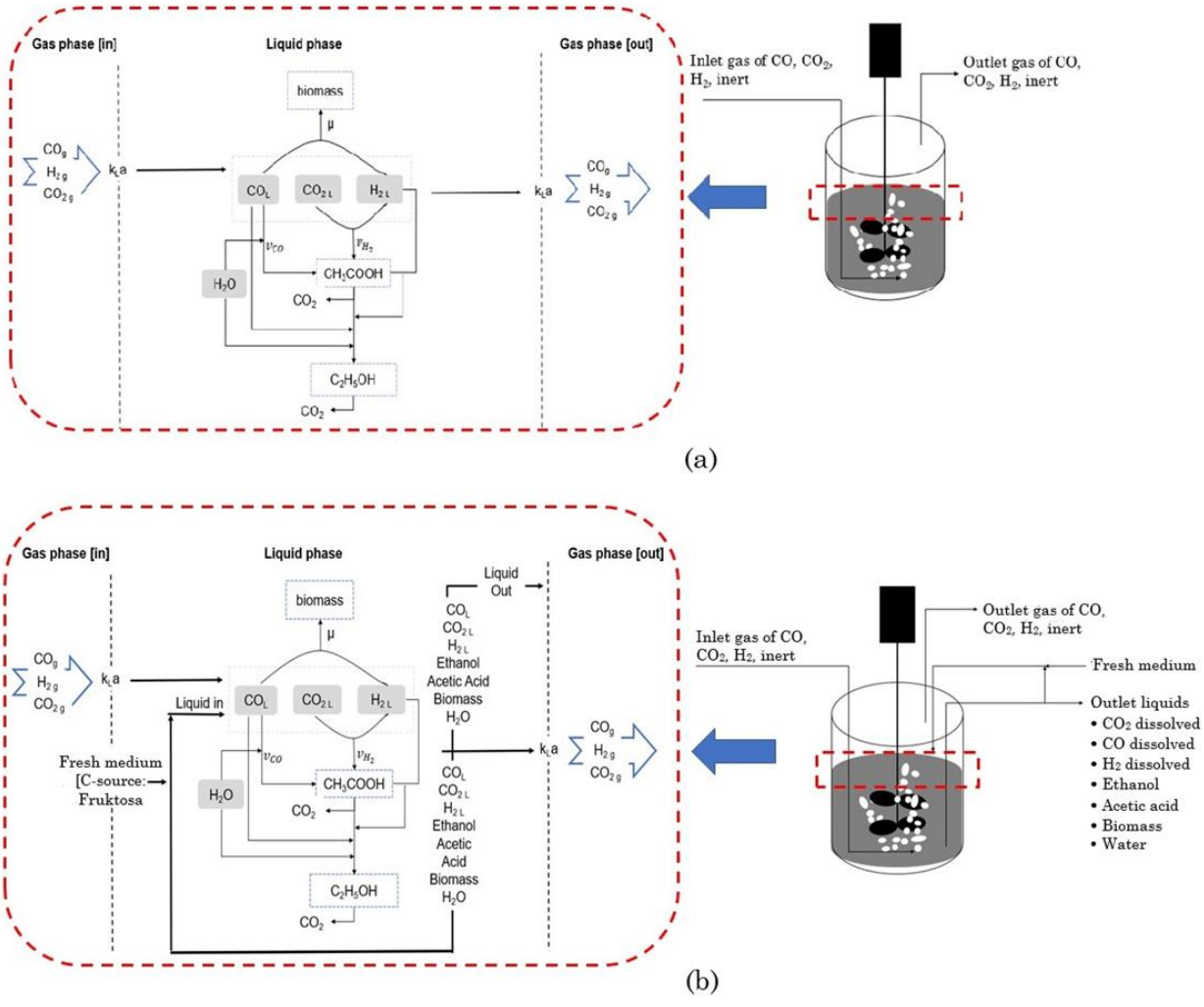

Figure 1. System model: (a) Batch, (b) Continuous

$$v_{CO} = -\frac{v_{max,CO} \cdot C_{L,CO}}{K_{S,CO} + C_{L,CO}} \cdot I_{Et} \cdot I_{Ac} \cdot I_{CO} \quad (5)$$

$$v_{H2} = -\frac{v_{max,H_2} \cdot C_{L,H_2}}{K_{S,H_2} + C_{L,H_2}} \cdot I_{Et} \cdot I_{Ac} \cdot I_{CO} \quad (6)$$

The inhibitions of ethanol, acetic acid, and CO uptake follow standard inhibition kinetics (Equations 7–9). The values of the inhibitor constants (K_I) for ethanol (K_{IE}), acetic acid (K_{IA}), and CO substrate (K_{ICO}) are taken from Medeiros [35].

$$I_{Et} = \frac{1}{1+\frac{C_{L,Et}}{K_{IE}}} \quad (7)$$

$$I_{Ac} = \frac{1}{1+\frac{C_{L,Ac}}{K_{IA}}} \quad (8)$$

$$I_{CO} = \frac{1}{1+\frac{C_{LCO}}{K_{ICO}}} \quad (9)$$

The specific growth rate of biomass (μ) is a function of the specific rates of CO and H_2 via yield coefficients $Y_{X.CO}$ and $Y_{X.H2}$ (Equations 10), and the death rate r_d is a function of cell concentration (C_x) (Equations 11). The values of $Y_{X.CO}$, $Y_{X.H_2}$ and the death constant (k_d) are taken from Medeiros [35].

$$\mu = -v_{CO}.Y_{X.CO} - v_{H_2}.Y_{X.H_2} \quad (10)$$

$$r_d = k_d.C_x \quad (11)$$

Acetic acid is produced from CO (Equation 1) and H_2/CO_2 (Equations 2). Ethanol is produced exlusively through reduction of acetic acid (Equations 3 and 4). The terms $F_{AcR,CO}$ and $F_{AcR,H2}$ are included solely for clarity in the equations and do not represent model parameters. The idea behind this set of equations is that acetic acid is reduced by its concentration (Equations 12 and 13). The values of $v^{CO}_{max,AcR}$, $v^{H2}_{max,AcR}$, $K^{CO}_{s,AcR}$ and $K^{H2}_{s,AcR}$ are taken from Medeiros [35].

$$F_{AcR,CO} = \frac{v^{CO}_{max,AcR} \cdot C_{L,Ac}}{K^{CO}_{s,AcR} + C_{L,Ac}} \quad (12)$$

$$F_{AcR,H2} = \frac{v^{H2}_{max,AcR} \cdot C_{L,Ac}}{K^{H2}_{s,AcR} + C_{L,Ac}} \quad (13)$$

The corresponding reaction rates for the production of ethanol and acetic acid are calculated using (Equations 14-17).

$$v^R_3 = \left(\frac{1}{2}\right)\left(\frac{2F_{AcR,CO}}{2F_{AcR,CO} + |v_{CO}|}\right)|v_{CO}| \quad (14)$$

$$v^R_4 = \left(\frac{1}{2}\right)\left(\frac{2F_{AcR,H2}}{2F_{AcR,H2} + |v_{H2}|}\right)|v_{H2}| \quad (15)$$

$$v^R_1 = -\frac{(v_{CO} + 2v^R_3)}{4} \quad (16)$$

$$v^R_2 = -\frac{(v_{H2} + 2v^R_4)}{4} \quad (17)$$

The total production rates of other components are calculated using (Equations 18–20):

$$v_{CO_2} = 2v^R_1 - 2v^R_2 + 2v^R_3 \quad (18)$$

$$v_{et} = v^R_3 + 2v^R_4 \quad (19)$$

$$v_{Ac} = v^R_1 + v^R_2 - v^R_3 - v^R_4 \quad (20)$$

The concentration fields, except for biomass concentration, refer to the gas phase ($C_{G,j}$) or liquid phase ($C_{L,j}$), and species type (non-condensable [*NC*] or condensable [*C*]), with V_G and V_L representing the volumes of gas and liquid inside the reactor (mL, L, or m^3), respectively. $Q_{G,in}$ and $Q_{G,out}$ are the gas volumetric flow rates (L/h) into and out of the vessel, Q_L is the liquid volumetric flow rate (L/h), $k_L a_j$ are mass transfer coefficients, and *XP* is the cell purge fraction, i.e., the fraction of cells that are not recycled to the vessel. The mass balance is shown in Equations 21– 24 as follows:

Gas phase:

$$\frac{dC_{G,j}}{dt} = \left(\frac{1}{V_G}\right).\left(Q_{G,in}C_{G,j,in} - Q_{G,out}C_{G,j}\right) - k_L a_j \left(\frac{C_{G,j}}{m_j} - C_{L,j}\right)\left(\frac{V_L}{V_G}\right) \quad (21)$$

Table 1. The parameters used in the modeling

Data	Component						Unit
	CO	CO_2	H_2	Ethanol	Acetic Acid	Water	
H_j (36^{0}C)	4.97e9	1.21e8	6.69e9	-	-	-	Pa
kLa	300.5	425.9	277.1	-	-	-	h^{-1}
P_{sat}	-	-	-	1.52e4	4.05e3	4.05e3	Pa
γ_j	-	-	-	7.6	3.5	-	-
υ_{max}	0.0463	-	0.0316	-	-	-	$mol.g^{-1}.h^{-1}$
K_s	1,15e-5	-	6,75e-4	-	-	-	$mol.L^{-1}$
K_l	1.36e-4	-	-	0.217	0.962	-	$mol.L^{-1}$
Y_x	0.754	-	0.201	-	-	-	$g.mol^{-1}$
v^{ACR}_{Max}	0.0242	-	1.76e-3	-	-	-	$mol.g^{-1}.h^{-1}$
K^{ACR}_s	0.388	-	0.464	-	-	-	$mol.L^{-1}$
K_d	0.00697						h^{-1}

Liquid phase:

$$\frac{dC_{L,j}}{dt} = k_L a_j \left(\frac{C_{G,j}}{m_j} - C_{L,j}\right) + v_j . C_x + \left(\frac{Q_L}{V_L}\right).\left(C_{L,j,in} - C_{L,j}\right) \quad (22)$$

$$\frac{dC_{L,k}}{dt} = -k_L a_k \left(\frac{C_{L,k}}{m_k} - C_{G,k}\right) + v_j . C_x + \left(\frac{Q_L}{V_L}\right).\left(C_{L,k,in} - C_{L,k}\right) \quad (23)$$

Biomass concentration:

$$\frac{dC_X}{dt} = \left(\frac{Q_L}{V_L}\right).\left(-C_X . XP\right) + \mu C_X - r_d \quad (24)$$

The volumetric exit gas flow is determined using a mole balance in the gas and liquid phases under isobaric conditions. The total moles of gas exiting the reactor are calculated using Equation 25, while the exit gas flow, Q, is calculated using the ideal gas law assumption in Equation 26.

$$N_{G,out}\left(\frac{mol}{hr}\right) = Q_{G,in}\Sigma_j C_{G,j,in} - \Sigma_{j\in NC}\left(k_L a_j \left(\frac{C_{G,j}}{m_{j\in NC}} - C_{L,j}\right)V_L\right) + \Sigma_{j\in C}(k_L a_j \left(\frac{c_{L,j}}{m_{j\in C}} - C_{G,j}\right)V_L) \quad (25)$$

$$Q_{G,out}\left[\frac{m^3}{hr}\right] = \frac{N_{G,out}RT}{P} \quad (26)$$

The value of the gas-liquid equilibrium factors, m_j and m_k, can be calculated using Equations 27 and 28, where R is the ideal gas constant (8.314 Pa.m^3/mol.K), MM_L and ρ_L refer to liquid phase molar mass (kg/mol) and density (kg/m^3), respectively, assuming pure water at 36 °C, H_j is Henry's law constant (Pa), $P_{sat,k}$ are the saturation pressures (Pa), and γ_k are the infinite-dilution activity coefficients. Symbol j for CO, CO_2, H_2, while k for ethanol and acetic acid.

$$m_j = \frac{H_j MM_L}{RT\rho_L} \quad (27)$$

$$m_k = \frac{\rho_L RT}{MM_L \gamma_k P_{sat,k}} \quad (28)$$

The dynamic fermentation model is defined by the ODEs in Equations 5-9. This model was simulated by using Matlab R2019b. The parameters used in the modeling are listed in Table 1 and Table 2 are operation condition. The effect of inlet syngas composition on fermentation metabolite-biomassa, acetic acid, and ethanol-was simulated using the inlet syngas composition outlined in Table 3 run A-E. The effect of *kLa* on fermentation metabolite-biomassa, acetic acid, and ethanol-was simulated using the variations in Table 3 run F-J. The standard gas composition consists of 55% CO, 10% CO_2, dan 20% H_2 [34].

The effect of fluctuation magnitude in inlet gas composition on the concentration of ethanol, acetic acid, and biomass was studied using Pattern 1 and 2, in which Pattern 1 gave an opposite fluctuation trend of Pattern 2. Pattern 1: CO and H_2 decrease during the first 4 days, remain standard for 4 days, increase for 4 days, and return to standard levels. CO_2 fluctuates inversely to CO and H_2 in both cases. Magnitude of fluctuation composition from the standard are

Table 2. Operating conditions (D_{cont} = Dilution rate continous operation; C_{biom} = Concentration of biomass in recycle process.

Parameters	Unit	Values
V_L	L	1
V_G	L	0.5
$Q_{G\ in}$	L.h^{-1}	1.2
T	K	310
P	atm	1
R	atm.L.mol^{-1}.K^{-1}	0.082
D_{cont}	h^{-1}	0.0035
C_{biom}	g.L^{-1}	1.187

Table 3. Variation of model simulation (*kLa* for CO_2 and H_2 is determined by comparing their values to CO, yielding 1.42 and 0.92, respectively.)

Run	CO (%)	CO_2 (%)	H_2 (%)	Inert (%)	Gas composition was taken from Ref.	*kLa* CO (h^{-1})	*kLa* value reference
A	55	10	20	15	[34]	300.5	
B	36	11	28	25	[42]	300.5	
C	25	20	15	40	[41]	300.5	[41]
D	19	19	41	21	[42]	300.5	
E	12	17	12	59	[29]	300.5	
F	55	10	20	15		40	[15]
G	55	10	20	15[a)]		108	[43]
H	55	10	20	15	[34]	216	[44]
I	55	10	20	15		300.5	[45]
J	55	10	20	15		1096.2	[46]

±5%, ±10%, ±15%, and ±20%. The effect of fluctuation duration in inlet gas composition on the concentration of ethanol, acetic acid, and biomass was analyzed for fluctuation duration variation 0.5, 1, 2, and 4 days. For this simulation the biggest flutuation magnitude (±20% from standard) was used in these simulation.

3. Results and Discussion

3.1 Effect of Syngas Composition Changes on Fermentation

The impact of syngas composition on batch fermentation was determined by altering the inlet gas composition, following Tabel 3 run A-E. The time profile of the batch fermentation is provided in the supplementary material for further reference. Because the total composition must equal 100%, changes in CO automatically affect CO_2 and H_2, therefore a gas ratio analysis is performed. The effect of inlet syngas composition on syngas fermentation performance was ilustrated in Figure 2.

3.1.1 CO Composition

Figure 2a shows that an increased CO concentration significantly boosts the production of these compounds. Indeed the calculated correlation coefficient for CO with ethanol, acetic acid, and biomass was very high (0.99 for ethanol and biomass, and 0.98 for acetic acid).

CO was the primary substrate in syngas fermentation. Thereby it was expected that increase in CO enhances the production of ethanol, acetic acid, and biomass. Carbon monoxide dehydrogenase (CODH) absorbed CO, converting it into CO_2 and electrons. These electrons were then transferred to ferredoxin (Fd) for ATP generation via the proton motive force (chemiosmotic coupling). The Acetyl-CoA pathway

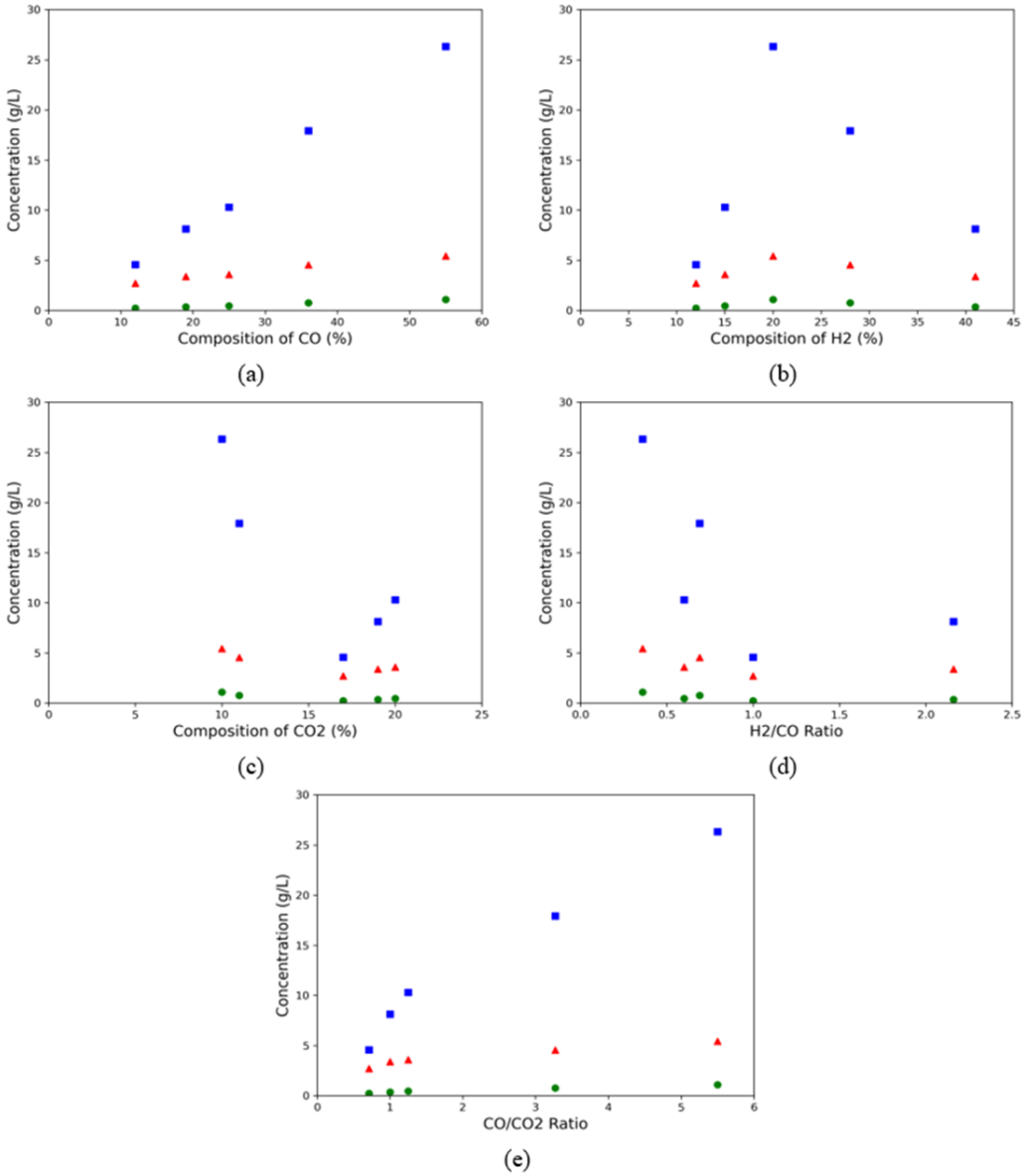

Figure 2. The effect of inlet syngas composition on syngas fermentation performance. ■ represents ethanol, ▲ represents acetic acid, and ● represents biomass.

produced acetyl-CoA, the precursor for ethanol and acetic acid. As CO serves as both a carbon and electron donor, elevated CO levels directly facilitated the synthesis of ethanol and acetic acid [36].

3.1.2 H_2 Composition

Figure 2b shows that while a peak in ethanol concentration was observed at 15-20% H_2, the overall trends indicated that product formation was not significantly enhanced by increasing H_2 composition. The correlation coefficients for H_2 with ethanol (0.02), acetic acid (0.10), and biomass (0.01) were all very low, indicating that a negligible relationship exists between H_2 composition and the production of these metabolites. These correlation data, along with the observed trends, suggested that other factors, rather than H_2 composition, were considered more critical in determining fermentation performance.

Hydrogen contributed to the reduction of CO_2 to acetyl-CoA, facilitating the production of valuable products such as acetic acid and ethanol. However, the weak correlations indicated that H_2 did not effectively promote acetyl-CoA formation in the presence of CO, likely due to inefficient electron transfer at high CO levels. H_2 did not significantly boost production, as microbes prefer CO as their main carbon and electron source [37]. Overall, H_2 did not enhance fermentation performance, highlighting its lower electron transfer efficiency compared to CO-derived pathways.

3.1.3 CO_2 Composition

Figure 2c shows that while ethanol and acetic acid concentrations increased with CO_2 composition, the overall trends indicated that further increases in CO_2 do not significantly enhance production. The correlation coefficients for CO_2 with ethanol (-0.853), acetic acid (-0.828), and biomass (-0.848) suggested a moderate to weak relationship, further indicating that CO_2 composition played a less critical role in the production of these metabolites. These trends and correlation data suggested that other factors, might be more influential in determining fermentation performance.

CO_2 could not provide reducing power on its own; it required H_2 as an electron donor. Insufficient H_2 levels hindered CO_2's effectiveness in fermentation. The reduction of CO_2 to acetyl-CoA depended on H_2, facilitated by the hydrogenase enzyme complex [38]. When CO_2 level was high and H_2 was low, acetogens struggled to reduce CO_2 to acetate or ethanol, which explained the negative correlation with CO_2 concentration.

3.1.4 H_2/CO Ratio

Figure 2d shows that as the H_2/CO ratio increases, the production of ethanol, acetic acid, and biomass decreases. These trends were consistent with the correlation coefficients for the H_2/CO ratio with ethanol (-0.59), acetic acid (-0.55), and biomass (-0.6), which indicated moderate negative relationships. This suggested that as the H_2/CO ratio increases, the production of these metabolites tent to decrease, reinforcing the idea that a higher H_2 proportion relative to CO may not be optimal for fermentation performance.

At an H_2/CO ratio of 1 or lower, CO availability might be insufficient for efficient acetyl-CoA synthesis. Acetogenic bacteria preferentially used CO over H_2 since CO provided both carbon and energy [36]. When H_2 level increased relative to CO without significant CO limitation, metabolism could become less efficient due to poor redox balance. Additionally, CO was crucial for energy conservation in acetogens, and its limitation at this ratio could decrease ATP production, thus slowing down ethanol production [39].

As the H_2/CO ratio exceeds 2, bacteria might undergo metabolic shifts to utilize H_2 more effectively as an electron donor, despite its lower efficiency compared to CO. While acetogens prefered CO, adequate H_2 facilitates CO_2 reduction via the Wood-Ljungdahl Pathway, aiding in ethanol production. This indicated that at higher H_2/CO ratios, microbes adapted their metabolism to increase H_2 use while sustaining ethanol output. Unlike Fischer-Tropsch synthesis, fermentation showed flexibility in H_2/CO ratios, allowing microbes to switch between CO utilization and H_2-mediated CO_2 reduction, though it still required sufficient CO availability [32].

3.1.5 CO/CO_2 Ratio

Figure 2e shows the relationship between the CO/CO_2 ratio and the production of ethanol, acetic acid, and biomass in syngas fermentation. As the CO/CO_2 ratio increased, the production of ethanol and acetic acid rose sharply. These trends were strongly supported by the high correlation coefficients of 0.99 for ethanol, 0.98 for acetic acid, and 0.99 for biomass. The high positive correlations indicated a strong relationship between the CO/CO_2 ratio and the production of these metabolites, suggesting that increasing the CO/CO_2 ratio significantly enhanced fermentation performance. This ratio ensured adequate CO for the Wood-Ljungdahl pathway, maximizing product formation. Thus, the CO/CO_2 ratio was crucial, emphasizing that CO availability was vital for optimal fermentation performance [36].

3.2. Effect of k_La on Fermentation

The efficiency of syngas fermentation relied on the effective dissolution and diffusion of CO, H_2, and CO_2 in the liquid phase. Table 4 presents data on the diffusivity and solubility of these gases. CO has a low solubility in water; thus, increasing mass transfer (higher *kLa*) enhanced its bioavailability, leading to better substrate utilization, increased biomass growth, and greater ethanol production. At low *kLa* values (40–108 h^{-1}), inadequate gas transfer limited CO availability, inhibiting microbial metabolism and resulting in lower biomass, acetate, and ethanol yields.

The experiment, conducted at 37 °C, benefited from higher gas diffusivity due to reduced water viscosity, facilitating faster gas movement. However, gas solubility decreased with rising temperatures, as molecules escaped the liquid phase more easily. Consequently, while elevated temperatures enhanced mass transfer, they also decreased the dissolved gas available for microbial metabolism.

At higher temperatures, the low solubility of CO, H_2, and CO_2 posed challenges for gas-liquid mass transfer in syngas fermentation. CO experienced greater mass transfer but reduced solubility, leading to lower dissolved concentrations and requiring increased *kLa* to maintain its availability. H_2, with its rapid diffusion yet low solubility, further complicated effective transfer. While CO_2 was the most soluble, its significant solubility declined at 37 °C could impact pH stability during fermentation. To counteract these effects, optimizing *kLa* was essential to ensure sufficient gas availability for microbial metabolism, ultimately supporting efficient ethanol production.

The effect of *kLa* on the batch syngas fermentation process was analyzed by varying *kLa* based on the bioreactor's configuration and operating conditions, as indicated in various studies, to predict ethanol production. The influence of *kLa* on metabolites is illustrated in Figure 3.

Figure 3 shows that higher *kLa* values enhanced metabolite production, indicating more active fermentation. This trend was supported by the correlation coefficients, with values of 0.80 for ethanol, 0.72 for acetic acid, and 0.86 for biomass, demonstrating a positive relationship between kLa and metabolite concentrations (Figure 3d). However, although increasing *kLa* significantly improved ethanol production during syngas fermentation, the results demonstrated that raising *kLa* from 300.5 h^{-1} to 1096.2 h^{-1} (a 3.5-fold increase) resulted in only a modest improvement in ethanol concentration, from approximately 24 $g.L^{-1}$ to 28 $g.L^{-1}$, rather than a proportional increase.

At lower *kLa* values, gas-liquid mass transfer was the primary limiting factor. In this condition, insufficient CO and H_2 were transferred into the liquid phase, leading to limited microbial growth and product formation [15]. However, beyond a certain threshold (around *kLa* 300 h^{-1}), the limitation shifted from mass transfer to microbial uptake and metabolism.

At high *kLa* levels, the increased substrate concentration led to saturation of the enzymes responsible for processing CO and H_2. Microbial enzymes, such as carbon monoxide dehydrogenase and hydrogenase, followed typical Michaelis-Menten kinetics. When substrate concentrations were low, increasing substrate availability increased the reaction rate. However, at high concentrations, these enzymes reached their maximum catalytic capacity (V_{max}), and further increased in substrate availability did not enhance reaction rates [40].

Table 4. Table 4. Data of diffusivity and solubility of CO, CO_2, and H_2 in water [47]. The diffusivity data at 25 °C, solubility data at 20 °C for CO and CO_2, and at 80 °C for H_2.

Gas	Diffusivity ($cm^2.s^{-1}$)	Solubility ($mg.L^{-1}$)
CO	1.8×10^{-5}	23.2
H_2	4.4×10^{-5}	8.5
CO_2	1.96×10^{-5}	901

3.3. Effects of Fluctuating Inlet Gas Composition in Syngas Fermentation

In the continuous fermentation method, the pH and temperature parameters were controlled, fresh substrate was continuously added to the bioreactor, while the resulting acetic acid and ethanol products were removed at the same rate, keeping the volume in the system constant. The initial phase of the simulation aimed to identify steady state conditions for ethanol and acetic acid, which were then set as initial values to assess the impact of syngas fluctuations on the fermentation process over 16 days. The continuous syngas fermentation process profile is illustrated in Figure 4. This research aimed to investigate the effects of fluctuating input syngas compositions on the continuous fermentation process. The disturbance included the magnitude and duration in inlet gas composition. According to Figure 4, the steady-state phase of ethanol and acetic acid was reached by the 40th day. However, in this simulation, day 50 (11.9 residence times) was used as the initial condition, with ethanol at 19.27 g/L, acetic acid at 2.28 g/L, and biomass at 0.96 g/L.

3.3.1 Effect of Fluctuation Magnitude

The disturbances imposed were 5%, 10%, 15%, and 20% from standard composition, which last over 4 days. Each disturbance magnitude followed a specific pattern: in Pattern 1, CO and H_2 decreased from days 4 to 8, return to normal from days 9 to 12, and then increased. Conversely, CO_2 was managed in the opposite manner. Pattern 2 operated inversely to Pattern 1, as illustrated in Figure 5a and b. The impact of the disturbance levels was depicted in Figure 5c-k.

The impact of disturbance levels in syngas composition on metabolite concentrations was illustrated in Figure 5. For ethanol production (Figure 5c-e), the results revealed that decreased CO availability in Pattern 1 led to a reduction in ethanol concentration, particularly prominent at higher disturbance levels (up to ±20%). Ethanol levels recovered as syngas composition returns to normal. In contrast, Pattern 2 showed an increase in ethanol production with higher CO and H_2 concentrations. The bar chart summary confirmed that ethanol concentration was positively influenced by increased CO availability and negatively impacted by CO reduction.

Similarly, acetic acid production followed the same trend (Figure 5f-h): reduced CO and H_2 concentrations in Pattern 1 resulted in lower acetic acid levels, while increased CO in Pattern 2 enhanced production. Biomass concentration

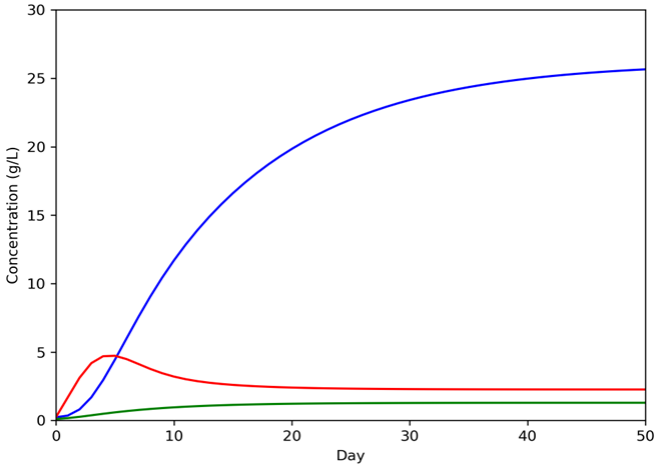

Figure 4. Profile of continuous fermentation results. — represents ethanol, — represents acetic acid, and — represents biomass.

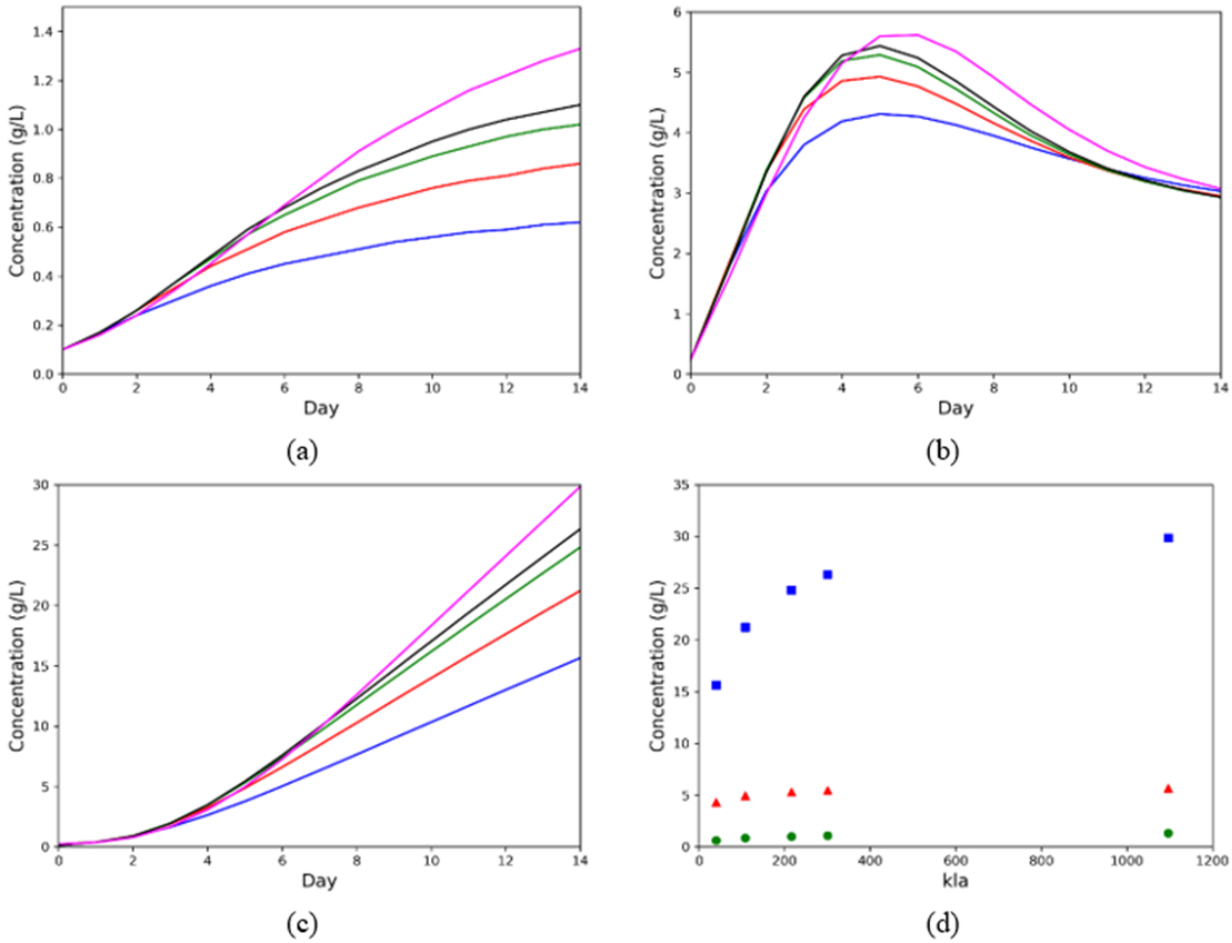

Figure 3. Profile of the Effect of *kLa* on Metabolites: (a) Biomass, (b) Acid Acetate, (c) Ethanol, (d) Combined Profile. — Run F (*kLa* CO 40 /h); — Run G (*kLa* CO 108 /h); — Run H (*kLa* CO 216 /hour); — Run I (*kLa* CO 300.5 /h); — Run J (*kLa* CO 1096.2 /h). In Figure (d), ■ ethanol, ▲ acetic acid, and ● biomass.

trends were consistent but display less sensitivity (Figure 5i-k). The percentage change in metabolite production increased or decreased proportionally with the magnitude of the disturbance in inlet gas composition, suggesting that larger fluctuations in gas composition had a greater impact on fermentation outcomes.

Across all metabolite profiles, the system did not achieve a steady state within the 4-day disturbance period. There was a clear delay in the system's response and recovery, and stabilization occured only after day 12 when syngas composition returned to normal. These findings highlighted the system's resilience to fluctuating feed conditions but also emphasized the need for sufficient stabilization time. These observations aligned with previous studies emphasizing that gas composition fluctuations significantly affected syngas fermentation outcomes [19].

3.3.2 Effect of Fluctuation Duration in Inlet Gas Composition on Fermentation

The impact of the duration of gas composition fluctuations on metabolite concentrations was illustrated in Figure 6. The duration varied at 0.5, 1, 2, and 4 days, with a maximum deviation of ±20% from the standard composition. Two fluctuation patterns were applied: Pattern 1, where CO and H_2 concentrations initially

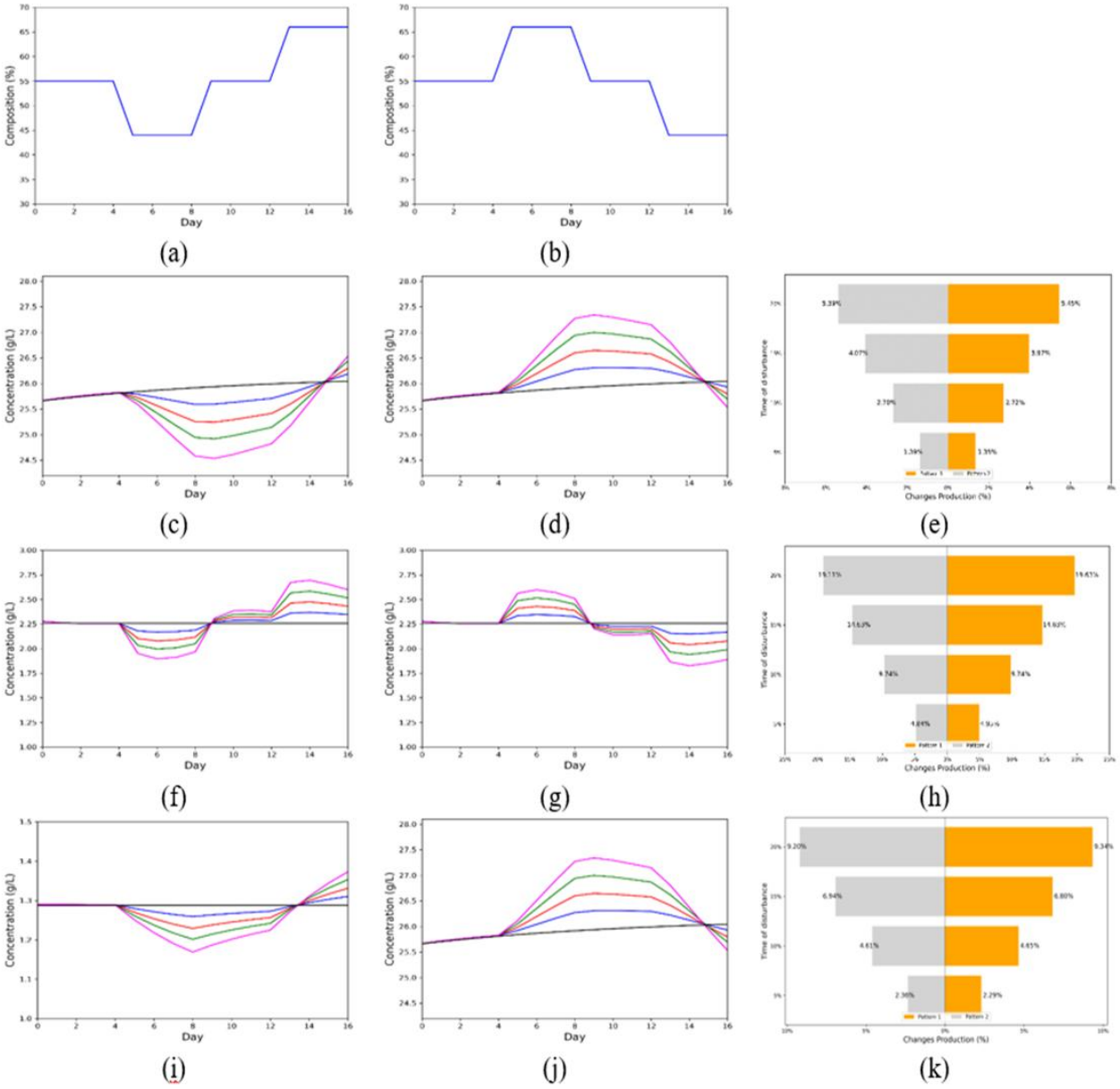

Figure 5. Effect of changes in syngas composition on concentration. (a) Composition of CO – Pattern 1, (b) Composition of CO – Pattern 2, (c) Ethanol – Pattern 1, (d) Ethanol – Pattern 2, (e) Ethanol – changes (orange pattern 1, grey pattern 2), (f) Acetic acid – Pattern 1, (g) Acetic acid – Pattern 2, (h) Acetic acid – changes (orange pattern 1, grey pattern 2), (i) Biomass – Pattern 1, (j) Biomass – Pattern 2, (k) Biomass – changes (orange pattern 1, grey pattern 2). Disturbance in syngas composition from standard composition: ±5% (—), ±10% (—), ±15% (—), ±20% (—), and standard composition (—).

decreased, returned to standard levels, then increased before stabilizing again; and Pattern 2, which operated inversely.

For ethanol production (Figure 6c-e), the results showed that shorter fluctuation durations (0.5 and 1 day) caused more frequent but smaller variations in concentration. Longer durations (4 days) resulted in larger amplitude changes, with ethanol levels decreasing during CO reduction phases in Pattern 1 and increasing during CO enrichment phases in Pattern 2. Figure 6e confirmed that longer fluctuation durations led to higher ethanol concentration, while shorter durations resulted in lower ethanol concentration.

Acetic acid production followed a similar trend. Reduced CO and H_2 concentrations in Pattern 1 led to lower acetic acid levels, while increased concentrations in Pattern 2 enhanced production. Larger acetic acid concentrations were observed for longer fluctuation durations, while shorter durations showed smaller concentration (Figure 6h). Biomass concentration trends were consistent with those of ethanol and acetic acid, though biomass showed less sensitivity (Figure 6i-k).

These results highlighted that longer fluctuation durations caused greater deviations in metabolite concentrations, while shorter

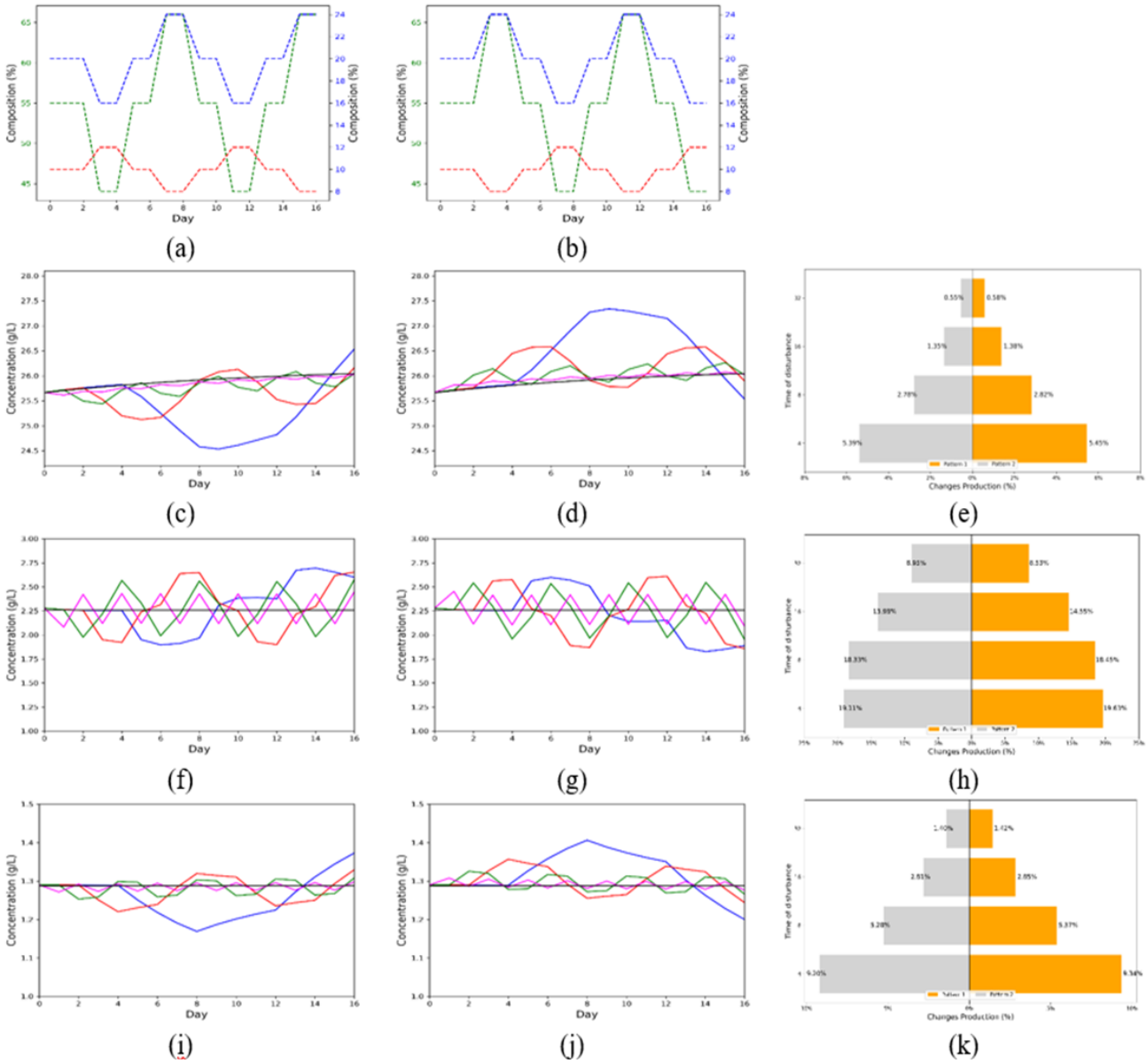

Figure 6. Impact of fluctuating inlet gas composition duration (±20% from standard) on syngas fermentation metabolite concentrations. (a) Gas composition changes every 2 days – Pattern 1 (- - : CO, - - : H_2, - - : CO_2), (b) Gas composition changes every 2 days – Pattern 2 (- - : CO, - - : H_2, - - : CO_2), (c) Ethanol - Pattern 1, (d) Ethanol - Pattern 2, (e) Ethanol changes, (f) Acetic acid - Pattern 1, (g) Acetic acid - Pattern 2, (h) Acetic acid changes, (i) Biomass - Pattern 1, (j) Biomass - Pattern 2, (k) Biomass changes. Different fluctuation durations are represented as follows: — (every 0.5 days), — (every 1 day), — (every 2 days), — (every 4 days), and — (standard composition).

durations allowed the system to adjust more rapidly, resulting in more stable fermentation outcomes. These findings aligned with previous studies emphasizing the importance of stable operating conditions and control strategies to mitigate the effects of fluctuating gas compositions [19].

Industries such as steel manufacturing, oil refining, and biomass gasification produce syngas with inherently variable compositions. The results suggest that syngas fermentation systems can be optimized to handle moderate fluctuations, improving cost-effectiveness by minimizing the need for gas stabilization. Additionally, microbial adaptability to different fluctuation patterns implies that a single fermentation system can process diverse gas sources, benefiting biorefineries that utilize various waste gases, including landfill gases, biomass-derived syngas, and industrial emissions, while maintaining consistent productivity.

4. Conclusion

This study examined the effects of syngas composition and its fluctuations on syngas fermentation performance using a kinetic model. In batch fermentation, increasing CO concentration was found to enhance ethanol, acetic acid, and biomass production, while higher H_2/CO ratios tended to reduce metabolite yields. Additionally, a higher CO/CO_2 ratio improved fermentation performance. In continuous fermentation, both the magnitude and duration of fluctuations in syngas composition influenced product concentrations, with larger and longer fluctuations causing more pronounced changes. However, the system demonstrated the ability to recover once the gas composition stabilized. These findings confirm that syngas composition and gas-liquid mass transfer (kLa) significantly affect fermentation outcomes, and that microbial systems exhibit resilience to temporary variations in gas input.

Acknowledgement

The author would like to thank the Ministry of Research, Technology, and Higher Education for supporting the BPP – DN scholarships in 2019 with contract number B/67/D.D3/KD.02.00/2019. This research was funded by Funding Assistance supported this research for State Universities Legal Entities (BP-PTNBH) Indonesian, Ministry of Research and Technology/National Research and Innovation Agency (BRIN) 2021 (PN-1) with contract number 2/E1/KP.PTNBH/2021.

CRediT Author Statement

Author Contributions: Noviani Arifina Istiqomah: Writing - original draft, Methodology, Investigation, Conceptualization. Rendy Mukti: Methodology and Formal analysis. Made Tri Ari Penia Kresnowati: Writing – review and editing, Project administration, and Funding acquisition. Tjandra Setiadi: Writing – review and editing, Supervision, and Funding acquisition. All authors have read and agreed to the published version of the manuscript.

References

[1] Dominguez-Ramos, A., Irabien, A. (2020). The role of power-to-gas in the European Union. *Green Chemical Engineering*, 1(1), 6–8. DOI: 10.1016/J.GCE.2020.10.002.

[2] Liew, F.M., Martin, M.E., Tappel, R.C., Heijstra, B.D., Mihalcea, C., Köpke, M. (2016). Gas Fermentation-A flexible platform for commercial scale production of low-carbon-fuels and chemicals from waste and renewable feedstocks. *Frontiers in Microbiology*, 7 (May) DOI: 10.3389/fmicb.2016.00694.

[3] Tse, T.J., Wiens, D..J., Chicilo, F., Purdy, S.K., Reaney, M.J.T. (2021). Value-Added Products from Ethanol Fermentation—A Review. *Fermentation*, 7, 4, 267. DOI: 10.3390/fermentation7040267

[4] Pedraza, L., Flores, A., Toribio, H., Quintero, R., Le Borgne, S., Moss-Acosta, C., Martinez, A. (2016). Sequential Thermochemical Hydrolysis of Corncobs and Enzymatic Saccharification of the Whole Slurry Followed by Fermentation of Solubilized Sugars to Ethanol with the Ethanologenic Strain Escherichia coli MS04. *Bioenergy Research*, 9(4), 1046–1052. DOI: 10.1007/s12155-016-9756-9.

[5] Devi, A., Niazi, A., Ramteke, M., Upadhyayula, S. (2021). Techno-economic analysis of ethanol production from lignocellulosic biomass–a comparison of fermentation, thermo catalytic, and chemocatalytic technologies. *Bioprocess and Biosystems Engineering*, 44(6), 1093–1107. DOI: 10.1007/s00449-020-02504-4.

[6] Sun, Y., Cheng, J. (2002). Hydrolysis of lignocellulosic materials for ethanol production: A review. *Bioresource Technology*, 83(1), 1–11. DOI: 10.1016/S0960-8524(01)00212-7.

[7] Foust, T.D., Aden, A., Dutta, A., Phillips, S. (2009). An economic and environmental comparison of a biochemical and a thermochemical lignocellulosic ethanol conversion processes. *Cellulose*, 16(4), 547–565. DOI: 10.1007/s10570-009-9317-x.

[8] Devarapalli, M., Journal, H.A.-B.R., 2015, U. (2015). A review of conversion processes for bioethanol production with a focus on syngas fermentation. *Biofuel Research Journal*, 7, 268–280.

[9] García-Aparicio, M.P., Ballesteros, I., González, A., Oliva, J.M., Ballesteros, M., Negro, M.J. (2007). Effect of Inhibitors Released During Steam-Explosion Pretreatment of Barley Straw on Enzymatic Hydrolysis. In: *Twenty-Seventh Symposium on Biotechnology for Fuels and Chemicals*. Humana Press, pp. 278–288.DOI: 10.1007/978-1-59745-268-7_22.

[10] Hidayatullah, I.M., Setiadi, T., Kresnowati, M.T.A.P., Boopathy, R. (2020). Xylanase inhibition by the derivatives of lignocellulosic material. *Bioresource Technology*, 300, 122740. DOI: 10.1016/J.BIORTECH.2020.122740.

[11] Zhang, Y., Ji, Y., Qian, H. (2021). Progress in thermodynamic simulation and system optimization of pyrolysis and gasification of biomass. *Green Chemical Engineering*, 2(3), 266–283. DOI: 10.1016/J.GCE.2021.06.003.

[12] Li, J., Li, L., Tong, Y.W., Wang, X. (2023). Understanding and optimizing the gasification of biomass waste with machine learning. *Green Chemical Engineering*, 4(1), 123–133. DOI: 10.1016/J.GCE.2022.05.006.

[13] Fang, Y., Paul, M.C., Varjani, S., Li, X., Park, Y.K., You, S. (2021). Concentrated solar thermochemical gasification of biomass: Principles, applications, and development. *Renewable and Sustainable Energy Reviews*, 150, 111484. DOI: 10.1016/J.RSER.2021.111484.

[14] Griffin, D.W., Schultz, M.A. (2012). Fuel and chemical products from biomass syngas: A comparison of gas fermentation to thermochemical conversion routes. *Environmental Progress & Sustainable Energy*, 31(2), 219–224. DOI: 10.1002/EP.11613.

[15] Munasinghe, P.C., Khanal, S.K. (2010). Syngas fermentation to biofuel: Evaluation of carbon monoxide mass transfer coefficient (kLa) in different reactor configurations. *Biotechnology Progress*, 26(6), 1616–1621. DOI: 10.1002/btpr.473.

[16] Philips, J., Rabaey, K., Lovley, D.R., Vargas, M. (2017). Biofilm formation by clostridium ljungdahlii is induced by sodium chloride stress: Experimental evaluation and transcriptome analysis. *PLoS ONE*, 12(1) DOI: 10.1371/journal.pone.0170406.

[17] Liu, K., Atiyeh, H.K., Tanner, R.S., Wilkins, M.R., Huhnke, R.L. (2012). Fermentative production of ethanol from syngas using novel moderately alkaliphilic strains of Alkalibaculum bacchi. *Bioresource Technology*, 104, 336–341. DOI: 10.1016/j.biortech.2011.10.054.

[18] Drake, H.L., Gößner, A.S., Daniel, S.L. (2008). Old acetogens, new light. *Annals of the New York Academy of Sciences*, 1125, 100–128. DOI: 10.1196/annals.1419.016.

[19] Daniell, J., Köpke, M., Simpson, S.D. (2012). Commercial biomass syngas fermentation. *Energies (Basel)*, 5:5372–5417.

[20] Jiang, Y., Guo, D., Lu, J., Dürre, P., Dong, W., Yan, W., Zhang, W., Ma, J., Jiang, M., Xin, F. (2018). Consolidated bioprocessing of butanol production from xylan by a thermophilic and butanologenic Thermoanaerobacterium sp. M5. *Biotechnology for Biofuels*, 11(1), 1–14. DOI: 10.1186/s13068-018-1092-1.

[21] Ramachandriya, K.D., Kundiyana, D.K., Wilkins, M.R., Terrill, J.B., Atiyeh, H.K., Huhnke, R.L. (2013). Carbon dioxide conversion to fuels and chemicals using a hybrid green process. *Applied Energy*, 112, 289–299. DOI: 10.1016/j.apenergy.2013.06.017.

[22] Sato, H., Matubayasi, N., Nakahara, M., Hirata, F. (2000). Which carbon oxide is more soluble? Ab initio study on carbon monoxide and dioxide in aqueous solution. *Chemical Physics Letters*, 323, 257-262. DOI: 10.1016/S0009-2614(00)00508-X.

[23] Mukti, R., Setiadi, T., Kresnowati, M.T.A.P. (2023). Challenges in Syngas Fermentation for Bioethanol Production: Syngas Composition. *Engineering Chemistry*, 1, 9-19. DOI: 10.4028/p-9g14o1.

[24] Abubackar, H.N., Veiga, M.C., Kennes, C. (2011). Biological conversion of carbon monoxide: Rich syngas or waste gases to bioethanol. *Biofuels, Bioproducts and Biorefining*, 5, 93–114. DOI: 10.1002/bbb.256.

[25] Phillips, J.R., Huhnke, R.L., Atiyeh, H.K. (2017). Syngas fermentation: A microbial conversion process of gaseous substrates to various products. *Fermentation*, 3(2). DOI: 10.3390/fermentation3020028.

[26] Gao, Y., Wang, M., Raheem, A., Wang, F., Wei, J., Xu, D., Song, X., Bao, W., Huang, A., Zhang, S., Zhang, H. (2023). Syngas Production from Biomass Gasification: Influences of Feedstock Properties, Reactor Type, and Reaction Parameters. *ACS Omega*, 8, 31620–31631. DOI: 10.1021/acsomega.3c03050.

[27] Ahmed, A., Cateni, B.G., Huhnke, R.L., Lewis, R.S. (2006). Effects of biomass-generated producer gas constituents on cell growth, product distribution and hydrogenase activity of Clostridium carboxidivorans P7T. *Biomass and Bioenergy*, 30(7), 665–672. DOI: 10.1016/j.biombioe.2006.01.007.

[28] Datar, R.P., Shenkman, R.M., Cateni, B.G., Huhnke, R.L., Lewis, R.S. (2004). Fermentation of biomass-generated producer gas to ethanol. *Biotechnology and Bioengineering*, 86(5), 587–594. DOI: 10.1002/bit.20071.

[29] Kundiyana, D.K., Huhnke, R.L., Wilkins, M.R. (2010). Syngas fermentation in a 100-L pilot scale fermentor: Design and process considerations. *Journal of Bioscience and Bioengineering*, 109(5), 492–498. DOI: 10.1016/j.jbiosc.2009.10.022.

[30] Kundiyana, D.K., Huhnke, R.L., Wilkins, M.R. (2010). Syngas fermentation in a 100-L pilot scale fermentor: Design and process considerations. *Journal of Bioscience and Bioengineering*, 109(5), 492–498. DOI: 10.1016/j.jbiosc.2009.10.022.

[31] Orgill, J.J., Lewis, R.S., Atiyeh, H.K. (2013). Syngas mass transfer analysis in a hollow fiber reactor. In: *Energy and Transport Processes 2013 - Core Programming Area at the 2013 AIChE Annual Meeting: Global Challenges for Engineering a Sustainable Future*. AIChE, p. 64.

[32] Jack, J., Lo, J., Maness, P.C., Ren, Z.J. (2019). Directing Clostridium ljungdahlii fermentation products via hydrogen to carbon monoxide ratio in syngas. *Biomass and Bioenergy*, 124, 95–101. DOI: 10.1016/j.biombioe.2019.03.011.

[33] de Medeiros, E.M., Posada, J.A., Noorman, H., Filho, R.M. (2019). Dynamic modeling of syngas fermentation in a continuous stirred-tank reactor: Multi-response parameter estimation and process optimization. *Biotechnology and Bioengineering*, 116(10), 2473–2487. DOI: 10.1002/bit.27108.

[34] Phillips, J.R., Klasson, K.T., Clausen, E.C., Gaddy, J.L. (1993). Biological Production of Ethanol from Coal Synthesis Gas Medium Development Studies. *Applied Biochemistry and Biotechnology*, 39, 559–571. DOI: 10.1007/BF02919018.

[35] de Medeiros, E.M., Posada, J.A., Noorman, H., Filho, R.M. (2019). Dynamic modeling of syngas fermentation in a continuous stirred-tank reactor: Multi-response parameter estimation and process optimization. *Biotechnology and Bioengineering*, 116(10), 2473–2487. DOI: 10.1002/bit.27108.

[36] Jeoung, J.H., Fesseler, J., Goetzl, S., Dobbek, H. (2014). Carbon monoxide. Toxic gas and fuel for anaerobes and aerobes: Carbon monoxide dehydrogenases. *Metal Ions in Life Sciences*, 14–113, 37–69. DOI: 10.1007/978-94-017-9269-1_3.

[37] Hermann, M., Teleki, A., Weitz, S., Niess, A., Freund, A., Bengelsdorf, F.R., Takors, R. (2020). Electron availability in CO2, CO and H2 mixtures constrains flux distribution, energy management and product formation in Clostridium ljungdahlii. *Microbial Biotechnology*, 13(6), 1831–1846. DOI: 10.1111/1751-7915.13625.

[38] Ragsdale, S.W., Pierce, E. (2008). Acetogenesis and the Wood–Ljungdahl pathway of CO2 fixation. *Biochimica et Biophysica Acta (BBA) - Proteins and Proteomics*, 1784(12), 1873–1898. DOI: 10.1016/j.bbapap.2008.08.012.

[39] Bertsch, J., Müller, V. (2015). Bioenergetic constraints for conversion of syngas to biofuels in acetogenic bacteria. *Biotechnology for Biofuels*, 8(1), 1-12. DOI: 10.1186/s13068-015-0393-x.

[40] Mohammadi, M., Najafpour, G.D., Younesi, H., Lahijani, P., Uzir, M.H., Mohamed, A.R. (2011). Bioconversion of synthesis gas to second generation biofuels: A review. *Renewable and Sustainable Energy Reviews*, 15(9), 4255–4273. DOI: 10.1016/j.rser.2011.07.124.

[41] Keryanti, Kresnowati, M.T.A.P., Setiadi, T. (2019). Evaluation of gas mass transfer in reactor for syngas fermentation. In: *AIP Conference Proceedings*. American Institute of Physics Inc. DOI: 10.1063/1.5094986.

[42] Carvalho, M.M.O., Cardoso, M., Vakkilainen, E.K. (2015). Biomass gasification for natural gas substitution in iron ore pelletizing plants. *Renewable Energy*, 81, 566–577. DOI: 10.1016/j.renene.2015.03.056.

[43] Riggs, S.S., Heindel, T.J. (2006). Measuring carbon monoxide gas-liquid mass transfer in a stirred tank reactor for syngas fermentation. *Biotechnology Progress*, 22(3), 903–906. DOI: 10.1021/bp050352f.

[44] Kapic, A., Jones, S.T., Heindel, T.J. (2006). Carbon monoxide mass transfer in a syngas mixture. *Industrial and Engineering Chemistry Research*, 45(26), 9150–9155. DOI: 10.1021/ie060655u.

[45] Anggraini, I.D., Keryanti, Kresnowati, M.T.A.P., Purwadi, R., Noda, R., Watanabe, T., Setiadi, T. (2019). Bioethanol production via syngas fermentation of clostridium ljungdahlii in a hollow fiber membrane supported bioreactor. *International Journal of Technology*, 10(3), 481–490. DOI: 10.14716/ijtech.v10i3.2913.

[46] Shen, Y., Brown, R., Wen, Z. (2014). Enhancing mass transfer and ethanol production in syngas fermentation of Clostridium carboxidivorans P7 through a monolithic biofilm reactor. *Applied Energy*, 136, 68–76. DOI: 10.1016/j.apenergy.2014.08.117.

[47] Green, D.W., and M.Z.S. (2019). *Perry's Chemical Engineers' Handbook*, 9th Edition. New York: McGraw-Hill Education.